The Plant Cell, Vol. 18, 598–611, March 2006, www.plantcell.org © 2006 American Society of Plant Biologists

Arabidopsis REGULATOR OF AXILLARY MERISTEMS1 Controls a Leaf Axil Stem Cell Niche and Modulates Vegetative Development [W]

Thomas Keller,[a] Jessica Abbott,[a] Thomas Moritz,[b] and Peter Doerner[a,1]

[a] Institute of Molecular Plant Sciences, School of Biological Sciences, University of Edinburgh, Edinburgh EH9 3JR, Scotland, United Kingdom

[b] Umeå Plant Science Centre, Department of Forest Genetics and Plant Physiology, Swedish University of Agricultural Sciences, SE-90187 Umeå, Sweden

Shoot branching is a major determinant of variation in plant stature. Branches, which form secondary growth axes, originate from stem cells activated in leaf axils. The initial steps by which axillary meristems (AMs) are specified and their stem cells organized are still poorly understood. We identified gain- and loss-of-function alleles at the *Arabidopsis thaliana REGULATOR OF AXILLARY MERISTEMS1* (*RAX1*) locus. *RAX1* is encoded by the Myb-like transcription factor MYB37 and is an *Arabidopsis* homolog of the tomato (*Solanum lycopersicum*) *Blind* gene. *RAX1* is transiently expressed in a small central domain within the boundary zone separating shoot apical meristem and leaf primordia early in leaf primordium development. *RAX1* genetically interacts with *CUP-SHAPED COTYLEDON* (*CUC*) genes and is required for the expression of *CUC2* in the *RAX1* expression domain, suggesting that *RAX1* acts through *CUC2*. We propose that *RAX1* functions to positionally specify a stem cell niche for AM formation. *RAX1* also affects the timing of developmental phase transitions by negatively regulating gibberellic acid levels in the shoot apex. *RAX1* thus defines a novel activity that links the specification of AM formation with the modulation of the rate of progression through developmental phases.

INTRODUCTION

Plant seedlings initially have a single growth axis for shoots and roots. Therefore, the diversity of plant stature observed in nature is largely due to two postembryonic processes: the formation of secondary growth axes and the timing of developmental phase transitions that govern meristem and, therefore, organ identity. Secondary growth axes require the establishment and activation of axillary meristems (AMs), which arise during modular plant growth in phytomers that comprise a leaf, an AM, and a stem segment. Once specified, rosette leaf AMs are activated in two patterns in *Arabidopsis thaliana*: an acropetal pattern of bud outgrowth, which is readily observed only in late flowering accessions, and a basipetal pattern of rosette paraclade formation upon the transition from vegetative growth to reproductive growth (Hempel and Feldman, 1994; Stirnberg et al., 1999; Grbic and Bleecker, 2000; Stirnberg et al., 2002). Once outgrowth has been activated, only a few cauline leaves are produced on the branch before its meristem forms an inflorescence.

The developmental origins of AMs have been controversial. On the basis of morphological and anatomical criteria, it has been proposed that the cells at the adaxial side of the boundary between incipient leaf primordium and shoot apical meristem (SAM) adopt AM fate de novo (Snow and Snow, 1942). Alternatively, it has been argued that these cells detach from the SAM early during leaf primordium development (Sussex, 1955). However, these arguments are based on morphology and do not take into account the complementary but distinct genetic functions required for meristem establishment and maintenance (Doerner, 2003). For example, studies with a molecular marker for indeterminate cell fate, such as *SHOOT MERISTEMLESS* (*STM*) (Long and Barton, 2000), have not clearly resolved the controversy because *STM* expression alone is insufficient to specify stem cell fate (Gallois et al., 2002; Lenhard et al., 2002), which requires coexpression of *WUSCHEL* (*WUS*) and possibly other genes of similar function (Haecker et al., 2004; Green et al., 2005).

Genetic approaches to identify the loci that control AM formation have proven powerful: Several genes have been identified in *Arabidopsis* and other model systems that control AM formation (for reviews, see McSteen and Leyser, 2005; Schmitz and Theres, 2005). *Lateral suppressor* (*Ls*) in tomato (*Solanum lycopersicum*) and its *Arabidopsis* and rice (*Oryza sativa*) homologs *LAS* and *MONOCULM1*, respectively, are required very early in AM development, as mutants lack any sign of AM development, including the stimulation of *STM* expression temporally associated with AM formation (Greb et al., 2003). *LAS* is expressed in the boundary zone separating the incipient leaf primordium from the SAM, similar to *CUP-SHAPED COTYLEDON* (*CUC*) and *LATERAL ORGAN BOUNDARY* (*LOB*) genes (Greb et al., 2003). This early onset of *LAS* expression suggests

[1] To whom correspondence should be addressed. E-mail peter.doerner@ed.ac.uk; fax 44-131-650-5392.
The author responsible for distribution of materials integral to the findings presented in this article in accordance with the policy described in the Instructions for Authors (www.plantcell.org) is: Peter Doerner (peter.doerner@ed.ac.uk).

[W] Online version contains Web-only data.

Article, publication date, and citation information can be found at www.plantcell.org/cgi/doi/10.1105/tpc.105.038588.

that the initial specification of a distinct AM identity occurs around the time of leaf primordium formation, possibly by maintaining cells in an indeterminate state as indicated by the *STM* marker. *CUC* genes may also play an important role in specifying AM identity as their overexpression stimulates adventitious shoot formation (Daimon et al., 2003), but the severe seedling phenotypes of hypomorphic *cuc* mutants has hindered detailed studies of their later functions in the plant life cycle. *LAS* encodes a putative transcription factor of the GRAS family. A further transcription factor required early in AM development was identified in tomato. The *Blind* (*Bl*) gene encodes a putative Myb-like transcription factor for which the *Arabidopsis* homolog has not yet been described. *bl* mutants lack AMs in many vegetative axils, and their response to SAM decapitation suggests that *Bl* is required early in AM development (Schmitz et al., 2002). Double mutants of *ls* and *bl* in tomato revealed additive phenotypes, suggesting the existence of at least two pathways involved in AM initiation (Schmitz et al., 2002).

Here, we report the identification of a gene we have designated *REGULATOR OF AXILLARY MERISTEMS1* (*RAX1*), which is encoded by the Myb-like transcription factor MYB37, and is the putative *Arabidopsis* homolog of the tomato *Bl* gene. We show that *RAX1* is expressed in a small central domain within the boundary zone separating SAM and leaf primordia during early leaf primordium development and is currently the earliest spatial marker for future AMs. *RAX1*, which is a transcriptional activator, genetically interacts with *CUC* genes and is required for the expression of *CUC2* in the *RAX1* expression domain. Our data suggest that *RAX1* promotes early stages of AM formation and functions to establish or maintain an environment conducive for stem cell organization in the course of AM formation. Hence, *RAX1* is involved in establishing the AM stem cell niche. *RAX1* also affects the timing of developmental phase transitions by negatively regulating gibberellic acid levels in the shoot apex.

RESULTS

A Dominant Mutant That Affects Branching

We generated a population of ~5000 activation-tagged individuals in the FA4C reporter gene background established in the Columbia (Col-0) ecotype (Colón-Carmona et al., 1999). Using the pSKI015 vector, which carries four outward-facing 35S enhancers adjacent to the left border (Weigel et al., 2000), we screened for individuals with altered growth and vegetative development. A dominant mutant with reduced rosette branching was identified. This mutant defined a locus designated *RAX1*, and we refer to the dominant allele as *rax1-1D*. We observed two phenotypic classes in segregating populations, which corresponded to the hemizygous or homozygous state of the *rax1-1D* allele (Figure 1), suggesting that the effects of this allele were dosage dependent.

When compared with the parental FA4C line (Figure 1A), hemizygous individuals, which we refer to as *rax1-1D*/+, were slightly dwarfed and formed compact rosettes with smaller, rounder, and slightly wrinkly leaves (Figure 1B). After the transition to flowering, these plants formed significantly fewer rosette branches than the wild type (Table 1). However, slightly more cauline paraclades were formed on the elongating inflorescence stem when compared with FA4C (Table 1). Hemizygous individuals then produced flowers on long pedicels and fertile seed; however, *rax1-1D*/+ plants produced fewer flowers than wild-type siblings (see Supplemental Figure 1 online). This data suggested that *RAX1* primarily regulates rosette branching.

rax1-1D homozygotes displayed a stronger phenotype that affected the shoot meristem: after germination, they were more dwarfed than *rax1-1D*/+ plants and never produced more than 6 to 10 leaves before arresting further development (Figure 1D). However, after a period of developmental stasis, some of these plants initiated new rosette branches of wild-type appearance (Figure 1E). These shoots eventually produced inflorescences with fertile flowers. However, this reversion was not permanent, as the progeny of these plants initially all displayed the severe phenotype.

To distinguish whether *rax1-1D*/+ individuals had defects in AM establishment or bud outgrowth, we examined axils in more detail by scanning electron microscopy. In wild-type FA4C plants, the first visible evidence of AM formation was the appearance of a cluster of small, proliferating cells at the basal end of the adaxial surface of the petiole (Figure 1F). Subsequently, these cells organized into an AM flanked by two leaf primordia (Figure 1G). In *rax1-1D*/+ plants, the field of small, proliferating cells was much enlarged laterally and distally into the petiole and frequently gave rise to more than one organizing center for an AM (Figures 1H and 1I). This suggested that *RAX1* activity promoted early steps of AM formation.

In plants homozygous for *rax1-1D*, the scanning electron microscopy analysis revealed that the SAM was consumed in the formation of a terminal leaf primordium or led to the formation of small, radially symmetric structures with leaf epidermal cell types (Figures 1K and 1L). However, in individuals where the severe phenotype did not persist, new shoots were produced in existing leaf axils (Figure 1M).

However, stimulation of AM formation by *RAX1* does not lead to increased rosette branching (Table 1). To test the hypothesis that the *rax1-1D* allele interfered with later stages of AM development or bud outgrowth, but not with the ability to specify and initiate AMs, we examined branching in plants that had been decapitated 2 weeks after the primary stem had begun to elongate. AMs are specified during vegetative development, but in *Arabidopsis*, buds are formed and branch outgrowth is activated only after the transition to flowering. The SAM suppresses branching, referred to as apical dominance (Cline, 1997). When *rax1-1D*/+ plants were decapitated, rosette branching increased strongly, while only a modest increase in branch number was seen in the wild type (Table 1). Overall branch number in these was very variable, and five of 22 decapitated *rax1-1D* individuals produced a much larger number of branches than the mean, suggesting that many more AMs were produced in this background. We concluded that *RAX1* promotes early steps of AM formation and that reduced rosette branching observed in *rax1-1D*/+ plants was due to interference with later steps.

rax1-1D Is a Hypermorphic Allele of a R2R3-Type Myb Gene

The *rax1-1D* phenotype cosegregated with BASTA resistance conferred by the pSKI015 activation tagging vector, indicating

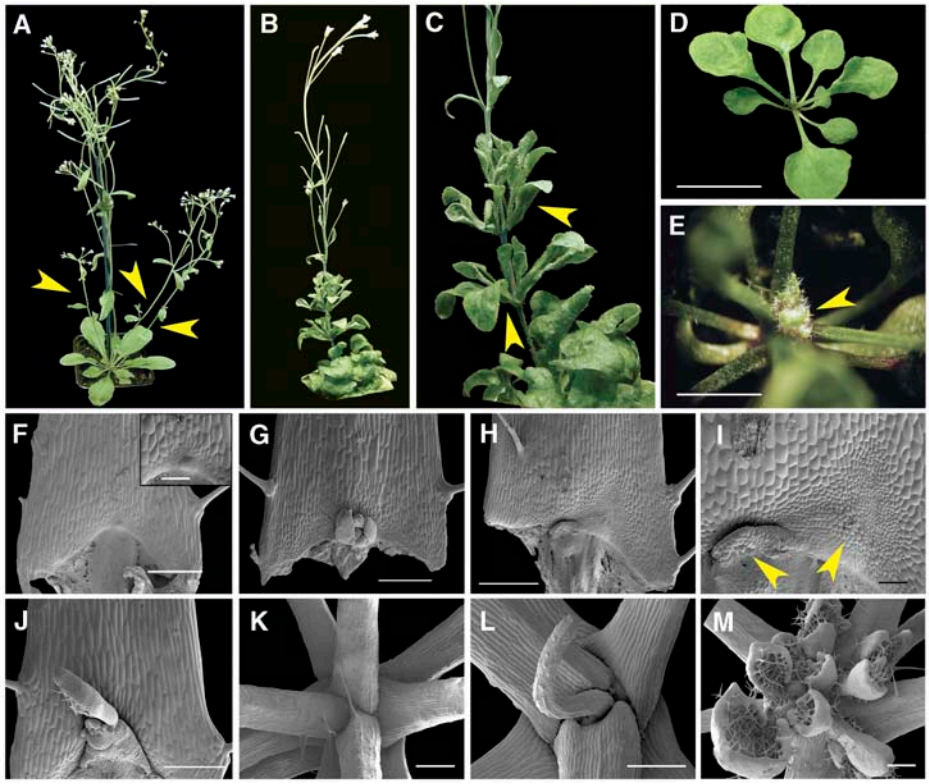

Figure 1. *rax1-1D*/+ Plants Establish Supernumerary AM Organizing Centers.

(A) Wild-type (FA4C) plant midway through reproductive development, showing three rosette paraclades (arrowheads).
(B) *rax1-1D*/+ plant at a similar stage in development, completely lacking rosette paraclades.
(C) Close-up of previous individual, showing aerial rosettes and continued production of leaves on branches originating from cauline leaf axils.
(D) *rax1-1D* homozygous plant. After producing 6 to 10 true leaves, *rax1-1D* homozygous seedlings cease leaf production. Many plants die after resting at this stage for 2 to 3 weeks.
(E) A variable fraction of *rax1-1D* homozygous seedlings regenerates a SAM from the axils of the youngest initially produced leaves. This panel shows an early stage of such plant.
(F) Scanning electron micrograph of rosette leaf axil in FA4C. The inset shows the central domain at the basal end of the petiole in higher magnification, revealing the initiation of an AM.
(G) Scanning electron micrograph of a developing rosette AM in the FA4C wild-type background.
(H) Scanning electron micrograph of rosette leaf axil in *rax1-1D*/+ with two organizing centers of AM formation.
(I) A magnified view of the same specimen shows a much larger population of small proliferating cells organizing into two centers (arrowheads).
(J) Scanning electron micrograph of rosette leaf axil in *rax1-1D*/+ treated with GA_3. GA_3 was sprayed twice-weekly during vegetative growth as a solution of 100 μM GA_3 and 0.02% Tween-20. AM development is further advanced, but branches did not develop.
(K) Scanning electron micrograph of a shoot apex of a plant similar to the one shown in **(D)**, showing that the SAM has been completely consumed in the process of leaf organogenesis.
(L) Scanning electron micrograph of a plant similar to the one shown in **(D)**, except that development of the final organ is incomplete.
(M) Scanning electron micrograph of plant similar to that shown in **(E)**, revealing the initiation of new AMs.
Bars = 1 cm in **(D)**, 2.5 mm in **(E)**, 500 μm in **(F)** to **(M)**, and 100 μm in **(F)** inset.

that the *RAX1* locus was tagged. To identify the site of T-DNA insertion in the genome, we used thermal asymmetric interlaced PCR (Liu et al., 1995). Plants carrying the *rax1-1D* allele carried a simple T-DNA insertion on chromosome 5, 2381 bp upstream of the start codon of the gene At5g23000 (Figure 2A), which encodes MYB37, a Myb-like transcription factor of the R2R3 class (Stracke et al., 2001). To confirm that MYB37 is *RAX1*, we examined the expression of genes flanking the T-DNA insertion site and recapitulated the insertion of the activation-tagging vector. While the expression of the C2H2-type putative transcription factor gene described by the At5g22990 gene model was unaffected by the presence of the T-DNA, RNA levels of MYB37 were strongly elevated in individuals carrying the *rax1-1D* allele (Figure 2B): MYB37 transcripts were undetectable in RNA gel blots with wild-type samples but accumulated to high levels in leaf and shoot apices of *rax1-1D* plants. RT-PCR analysis revealed that MYB37 was not expressed in wild-type leaves (see Supplemental Figure 2 online), suggesting that this gene was ectopically expressed in leaves of plants carrying the *rax1-1D* allele. Interestingly, MYB37 transcript abundance was much

reduced in the leaves of *rax1-1D* homozygous plants in which the severe phenotype did not persist, suggesting that very-high-level MYB37 expression was important for the *rax1-1D* phenotype. To test whether we could recreate *rax1-1D* phenotypes, we generated a construct encompassing four 35S enhancer elements, the putative MYB37 promoter, MYB37 gene, and 3′ terminator sequences. This was introduced into wild-type *Arabidopsis*, and 126 transformants were phenotypically analyzed. Approximately 20% of transformants recapitulated the *rax1-1D* hemizygous and homozygous phenotypes. The low frequency of phenotypic plants was not surprising, considering that MYB37 expression levels would have to be very high to manifest the hemizygous and homozygous phenotypes. We concluded that the *rax1-1D*/+ *and rax1-1D* phenotypes were caused by insertion of the activation tagging T-DNA upstream of MYB37 and, hence, that *RAX1* was MYB37.

MYB37 is closely related to several other R2R3 Myb genes in *Arabidopsis* as well as the recently identified *Bl* gene, which regulates sympodial branching in tomato (Stracke et al., 2001; Schmitz et al., 2002). MYB37 is most closely related to MYB38 (At2g36890) and tomato *Bl* (Figure 2C). The genetic function of most members of this clade is currently unknown, but MYB68 (At5g65790) is expressed in roots and is required for normal root growth (Feng et al., 2004). We therefore aimed to examine *RAX1* genetic function by identifying loss-of-function alleles.

Loss of RAX1 Function Reduces AM Formation and Branching

To characterize *RAX1* genetic function, we screened available T-DNA insertion collections. We identified the recessive *rax1-2* allele in the Wassilewskija (Ws-2) background (Krysan et al., 1999). This allele carries a T-DNA insertion in the second MYB37 intron (Figure 2A). Using RNA gel blot analysis, we could not detect *RAX1* transcripts in samples extracted from wild-type

Table 1. Branching in Wild-Type and *rax1-1D*/+ Plants

	FA4C (*n*)	*rax1-1D*/+ (*n*)
Rosette branches with IM	5.41 ± 0.18 (29)	1.11 ± 0.17* (28)
Cauline branches with VM	0.03 ± 0.15 (29)[a]	2.11 ± 0.48* (28)
Cauline branches with IM	4.83 ± 0.15 (29)	5.82 ± 0.31* (28)
Total branches	10.24 ± 0.25 (29)	9.04 ± 0.51** (28)
Rosette branches with IM after decapitation	6.9 ± 0.37 (17)	6.6 ± 1 (21)

Branches with an inflorescence meristem at the apex (branches with IM) are distinguished from branches with vegetative identity that produce leaves only (branches with VM). Rosette branches originate from axils on the unexpanded stem, while cauline branches originated from the expanded segment of the stem. Errors are standard errors of the mean. One asterisk indicates significant differences ($P < 0.01$), while two asterisks indicates significant differences ($P < 0.05$) identified with Student's *t* test. Numbers in parentheses indicate the number of individuals tested.

[a] One individual produced a single cauline branch with several leaves arranged as an aerial rosette.

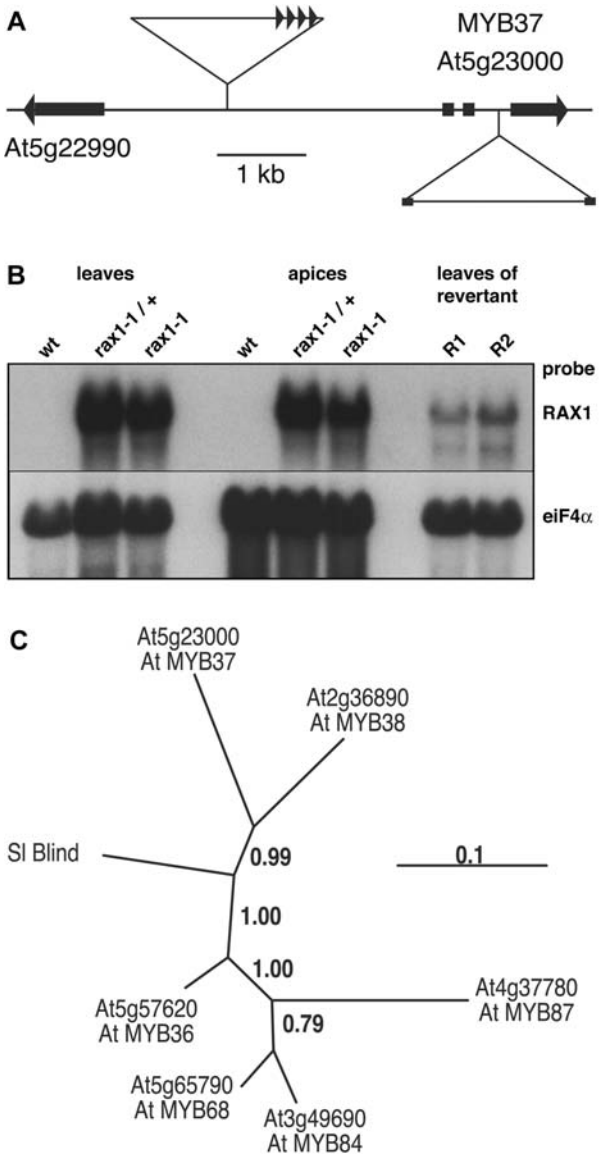

Figure 2. *RAX1* Is a Putative Myb-Like Transcription Factor Expressed at Low Levels.

(A) Schematic of genome organization around the At5g23000 gene model for MYB37. The orientation of the four 35S enhancer repeats in the activation-tagging T-DNA 2381 bp 5′ of the MYB37 start codon is indicated by triangles. The insertion site of the T-DNA inserted in the second intron of MYB37 is indicated below.

(B) *RAX1* expression is very high in *rax1-1D*. RNA was extracted from leaves and microdissected shoot apices of *rax1-1D* hemizygous or homozygous individuals and from *rax1-1D* homozygous revertants. RNA gel blot analysis shows high levels of *RAX1* RNA in *rax1-1D* individuals and much reduced levels in leaves of revertant homozygous *rax1-1D* plants. A 501-bp *RAX1*-specific probe corresponding to the third exon was used to detect *RAX1* transcripts, and RNA loading was checked by hybridization to eukaryotic translation initiation factor 4A (*eIF-4A*) transcripts.

(C) Phylogenetic relationship between closely related *Arabidopsis* and tomato (Sl) Myb genes. The scale for branch lengths indicates the number of substitutions per amino acid residue. Genes are designated in accordance with the accompanying article.

(Figure 2B) or *rax1-2* shoot apices. We therefore used RT-PCR with two sets of primers, corresponding to targets 5′ or 3′ of the T-DNA insertion, to assess whether *rax1-2* was a null allele. *RAX1* expression could not be detected with either primer set in samples isolated from *rax1-2*, while it was readily detected in samples from Ws-2 (see Supplemental Figure 3 online). Therefore, *rax1-2* is a null allele. We identified a further line (SALK_009859) in the SALK collection (Alonso et al., 2003) with a T-DNA insertion at the 3′ end of the gene, but homozygous individuals had only modestly reduced *RAX1* RNA levels and no detectable phenotype. This line was not further characterized.

Individuals hemizygous for *rax1-2* had no detectable phenotype, but homozygous *rax1-2* plants had a branching phenotype: when grown in long- (LD) or short-day (SD) conditions, they produced fewer paraclades from rosette and cauline leaf axils when compared with the Ws-2 wild type (Table 2, Figures 3A to 3E). The phenotype was slightly more pronounced in SD (Table 2). The rosette paraclade phenotype of *rax1-2* was less severe than that of *rax1-1D*/+ (Table 1). In contrast with *rax1-1D*/+ plants, the small clusters of proliferating cells characteristic for the early stages of AM formation were completely absent in most rosette or cauline leaf axils when analyzed by scanning electron microscopy (Figures 3F and 3G), confirming that *RAX1* is required early in AM formation. Consistent with this interpretation, decapitated *rax1-2* plants did not show increased branching (Table 2), as was seen for *rax1-1D*/+ (Table 1). Homozygous *rax1-2* plants also produced fewer flowers than the matching wild type (see Supplemental Figure 1 online).

To unambiguously show that the *rax1-2* allele was responsible for the phenotypes observed, we complemented the mutant by introduction of a wild-type copy of the *RAX1* gene into *rax1-2* homozygous plants. We obtained 52 transformed lines, of which 15 segregated a single T-DNA, and analyzed branching in two lines in more detail: In this experiment, the Ws-2 wild type produced 3.1 ± 0.27 rosette paraclades, while in *rax1-2*, 1.6 ± 0.24 rosette paraclades were made. The *rax1-2* lines transformed with a wild-type copy of *RAX1* formed 3.3 ± 0.28 and 3.2 ± 0.29 rosette paraclades, respectively, which was significantly different from the *rax1-2* line ($P < 0.001$), but not different from Ws-2. We concluded that the phenotypes observed in *rax1-2* were due to the insertional inactivation of *RAX1*.

Table 2. Branching in Wild-Type and *rax1-2* Plants

	Ws-2 (*n*)	*rax1-2* (*n*)
Rosette branches with IM (LD)	4.1 ± 0.15 (24)	2.4 ± 0.17* (24)
Cauline branches with IM (LD)	2.8 ± 0.10 (24)	2.9 ± 0.10 (24)
Rosette branches with IM (SD)	6.1 ± 0.20 (43)	3.1 ± 0.27* (63)
Cauline branches with IM (SD)	7.3 ± 0.13 (43)	4.0 ± 0.18* (63)
Rosette branches with IM after decapitation (SD)	6.7 ± 0.33 (15)	3.1 ± 0.27* (18)

Plants were grown in the photoperiodic conditions indicated. Rosette branches originate from axils on the unexpanded stem, while cauline branches originated from the expanded segment of the stem. Only branches topped by inflorescence meristems (IM) were observed. Errors are standard errors of the mean, and the asterisks indicate significant differences ($P < 0.01$) identified with Student's *t* test. Numbers in parentheses indicate the number of individuals tested.

Taken together, our data show that the *rax1-1D* and *rax1-2* alleles of *RAX1* have opposite effects on AM formation, and we conclude that *RAX1* promotes early steps in AM formation, such as the specification of axillary identity or of meristematic competence in axillary cells.

RAX1 Is Expressed Transiently in the Axils of Leaf Primordia

To establish how *RAX1* promoted early steps in AM formation, we examined *RAX1* expression and identified target genes. Using RT-PCR, we consistently detected *RAX1* expression in shoots. In shoots, the *RAX1* temporal expression pattern was biphasic. Low-level expression was observed from germination onward, but higher-level expression was restricted to the adult vegetative phase and became detectable upon initiation of the fifth leaf primordium, at the onset of the adult vegetative phase in Col-0 (Telfer et al., 1997) (Figure 4A). *RAX1* is expressed transiently during leaf primordium development (Figures 4B to 4G) in a small domain at the center of the boundary between the SAM and developing leaf primordia (Figures 4D to 4G), marking the position of cells competent to initiate AMs in the axils of the primary shoot (Figure 3H). A similar pattern of expression is recapitulated in AMs (Figure 4H) after the formation of the lateral bud and stimulation of its outgrowth at the transition to flowering. Consistent with the results of decapitation experiments (Tables 1 and 2), this suggested that *RAX1* functions early in AM development.

Early AM development depends on the specification of axillary identity and the maintenance of meristematic competence in such cells (Schmitz and Theres, 2005). We therefore examined expression of *LAS* (Greb et al., 2003) and *CUC* genes (Aida et al., 1999), which are expressed at the boundary zone between the SAM and leaf primordia and are required for axillary or shoot meristem formation, respectively. The expression pattern of *LAS* was unaffected in *rax1-2* plants when compared with the wild type (see Supplemental Figure 4 online).

By contrast, *CUC2* expression, normally observed in a continuous band separating the SAM from incipient leaf primordia (Figure 4I), was absent at the position of future AM initials in the *rax1-2* background (Figure 4J), precisely where *RAX1* is expressed (Figure 4F). Moreover, *CUC2* transcript levels were consistently reduced in *rax1-2* (Figure 4K). Precise regulation of *CUC* gene expression patterns is required for maintenance of the boundary between meristems and leaf primordia (Laufs et al., 2004). Together, these data indicate that *RAX1* is needed to promote *CUC2* expression in a central domain of boundary cells in leaf axils. By contrast, expression of *CUC3* was not affected (see Supplemental Figure 4 online).

CUC genes act through *STM* (Aida et al., 1999), which is also a potential target of *LAS* (Greb et al., 2003). Therefore, we examined the spatio-temporal pattern of *STM* transcript accumulation in the boundary zone between SAM and leaf primordia. STM expression in this zone is dynamic and complex (Long and Barton, 2000; Greb et al., 2003). Upon stimulation of AM activity, *STM* transcripts initially accumulated in a small group of cells at

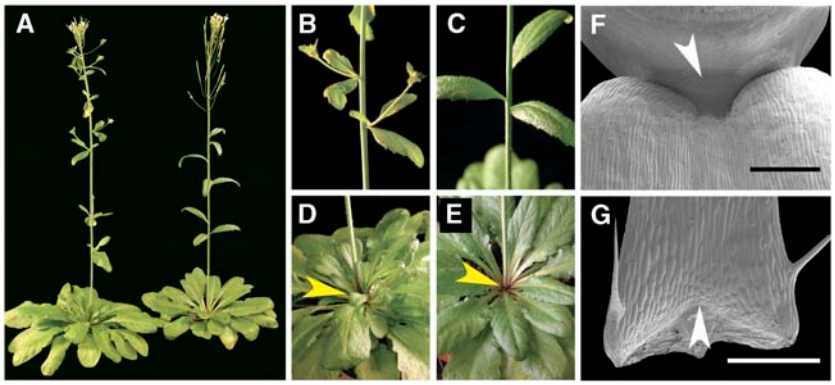

Figure 3. *rax1-2* Plants Develop Less Rosette and Cauline Branches and Cannot Initiate or Maintain an AM.

(A) Wild-type (Ws-2) plant early during reproductive development (left) and *rax1-2* plant at a similar developmental stage (right).
(B) to **(E)** Close-ups of the plants shown in **(A)**.
(B) Ws-2 wild-type inflorescence stem showing developing cauline branches.
(C) Inflorescence stem of *rax1-2* showing the absence of branches originating from cauline leaf axils.
(D) Ws-2 wild-type rosette with developing rosette paraclade (arrowhead).
(E) Rosette of *rax1-2* plant lacking rosette paraclade (arrowhead).
(F) Scanning electron micrograph of a barren *rax1-2* cauline leaf axil lacking an organizing center with proliferating cells (arrowhead).
(G) Scanning electron micrograph of barren rosette leaf axil in *rax1-2* lacking an organizing center with proliferating cells (arrowhead). Bars = 500 μm in **(F)** and **(G)**.

the base of leaf primordia in Ws-2 wild type (Figure 4L) and in *rax1-2* (Figure 4M) apices. By contrast, *STM* does not accumulate at this position in a *las* background (Greb et al., 2003). However, while in the wild type, *STM* expression continued as AMs were activated, *STM* expression in *rax1-2* did not persist, consistent with the notion that *rax1-2* axils do not maintain meristematic cells. These observations support the notion that *Ls* (the *LAS* homolog in tomato) and *Bl* (a Myb gene closely related to *RAX1*; Figure 2C) are in two separate genetic pathways (Schmitz et al., 2002).

We also examined the expression of *WUS*, which mediates stem cell niche functions to control stem cell population size. The spatial pattern of *WUS* expression in FA4C (Figure 4N) and *rax1-1D*/+ (Figure 4P) SAMs was very similar. In contrast with the tightly focused *WUS* transcript accumulation in FA4C AMs (Figure 4O), the *WUS* expression domain in *rax1-1D*/+ AMs was larger (Figures 4Q to 4S) and frequently gave rise to two discrete foci (Figure 4S), suggesting the presence of supernumerary AM organizing centers, similar to those observed by scanning electron microscopy (Figures 1H and 1I).

To test whether *CUC2* was an important target of the *RAX1* pathway, we examined whether a reduction of *CUC* gene dosage would enhance the severity of the *rax1-2* phenotype. Rosette paraclade formation in plants with reduced *CUC* gene dosage was indistinguishable from the wild type when in a *RAX1* background ($P > 0.1$). However, in a *rax1-2* background, rosette paraclade formation was dependent on *CUC* activity: progressive reduction of *CUC* gene dosage strongly enhanced the *rax1-2* branching phenotype (Table 3). These data supported the notion that *RAX1* acts through *CUC* genes. Based on the phenotype of *rax1-2*, its very early expression in leaf axils (Figures 4B to 4F), and the spatial pattern of expression (Figures 4E and 4J), we conclude that *RAX1* is required to establish or maintain a stem cell niche for AM formation by spatial control of *CUC2* expression.

RAX1 Is a Transcriptional Activator

Reduced *CUC2* expression in *rax1-2* homozygous individuals suggested that *RAX1* could be a transcriptional activator. We therefore examined the biochemical mechanism of *RAX1* function in a heterologous yeast system. Myb-like genes comprise two domains: an N-terminal DNA binding domain (DBD) and a C-terminal activating or repression domain. We fused the entire coding sequence downstream of the Myb DBD to the yeast *GAL4* DBD. As controls, similar constructs were made with the strong activating domain of the tomato THM18 Myb-like gene and the repression domain of the *Arabidopsis* MYB4 (At4g3620) gene (Schwechheimer et al., 1998; Jin et al., 2000). After these constructs were introduced into yeast cells, we analyzed their ability to transactivate expression of a β-galactosidase reporter gene. The *RAX1* C-terminal domain transactivated reporter gene expression, albeit to only 25% of the levels observed with the strong THM18 activation domain (Figure 5). We concluded that *RAX1* is a transcriptional activator.

RAX1 Modulates Progression through the Vegetative Phase and Affects GA Levels

In addition to rosette branching, hemizygous *rax1-1D*/+ and homozygous *rax1-2* plants differed from wild-type plants in vegetative development: *rax1-1D*/+ hemizygous plants had an extended vegetative phase, while by contrast, vegetative development in SD conditions was shorter in homozygous *rax1-2* plants (Table 4).

In *rax1-1D*/+ plants, time to flowering was almost twice as long compared with FA4C in LD or SD conditions (Table 4). These dwarfed plants produced more and darker green leaves than the wild type and did so at a higher rate (Table 4). Furthermore, the transition between vegetative and reproductive phases was

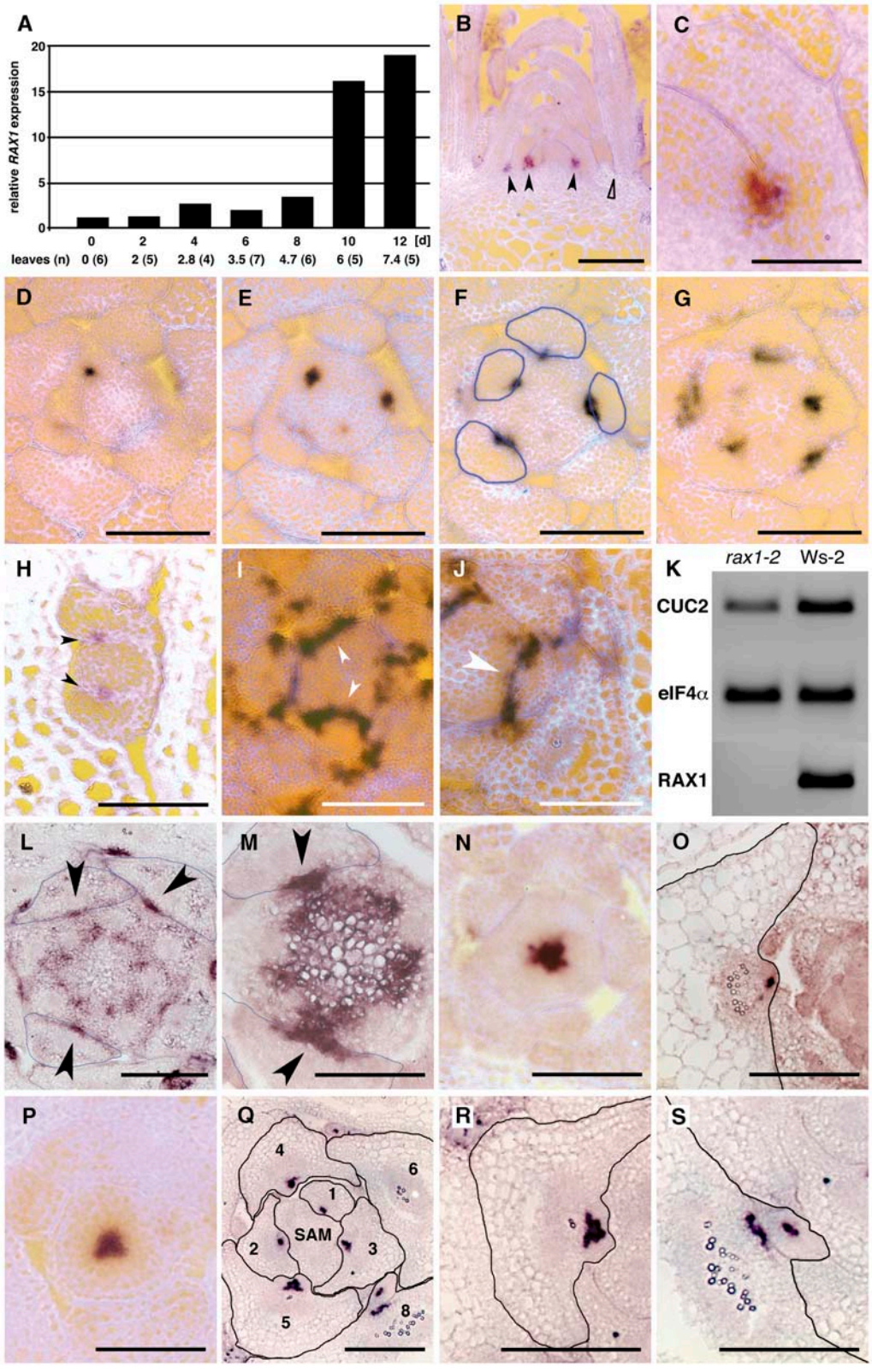

Figure 4. *RAX1* Is Transiently Expressed during Adult Vegetative Development in Young Leaf Primordia in a Pattern That Anticipates Future AM Position.

Table 3. Gene Dosage of *CUC* Genes Affects Branching in *rax1-2*

Genotype	L*er* (*n*)	*rax1-2* (*n*)
CUC1/*CUC1*, *CUC2*/*CUC2*	4.54 ± 0.22 (54)	2.0 ± 0.15* (72)
cuc1/*cuc1*, *CUC2*/*CUC2*	4.65 ± 0.27 (17)	0.4 ± 0.11* (40)
cuc1/*cuc1*, *cuc2*/*CUC2*	4.81 ± 0.22 (42)	0.08 ± 0.04* (60)

Plants were grown in SD conditions. Errors are standard errors of the mean, and the asterisks indicate significant differences ($P < 0.0001$) identified with Student's *t* test. Numbers in parentheses indicate the number of individuals tested. L*er*, Landsberg *erecta*.

protracted, exemplified by formation of aerial rosettes and cauline branches topped by meristems continuing to form leaves without formation of inflorescences (Figures 1B and 1C). Wild-type plants generally do not form such branches. These phenotypes suggested that *rax1-1D*/+ plants maintained vegetative identity and, hence, generated vegetative features after the onset of stem elongation. By contrast, in SD conditions, *rax1-2* individuals flowered ~10% earlier than Ws-2 after having produced ~20% less leaves (Table 4). Hence, in SD, *rax1-2* produces leaves at a lower rate than the wild type. Furthermore, these leaves were paler green than those in wild-type plants. Together, these data suggested that, in addition to regulating AM formation in rosettes, *RAX1* promoted vegetative meristem identity during *Arabidopsis* development. *RAX1* modulates the adult phase of vegetative development, as the duration of the juvenile phase was not significantly altered in *rax1-1D*/+ or *rax1-2* plants (see Supplemental Figure 5 online).

In light of the conditional effect of *rax1-2* on flowering time and the differences in leaf pigmentation, we examined whether *RAX1* activity affects gibberellic acid (GA) accumulation or responses in the shoot apex. GA promotes vegetative phase transitions and in *Arabidopsis* steadily accumulates during the adult vegetative phase toward a critical threshold sufficient to activate the transition to flowering (Blazquez et al., 1998; Simpson and Dean, 2002) mediated by *LEAFY* (*LFY*) expression (Blazquez et al., 1998). Moreover, GA is necessary for flowering in SD conditions (Wilson et al., 1992).

We first examined *LFY* transcript abundance, which responds to GA levels, in *rax1-1D*/+ individuals throughout vegetative development. *LFY* expression in *rax1-1D*/+ plants was strongly downregulated during vegetative development (Figure 6A). We then genetically tested the link between *RAX1* and *LFY* activity using the *lfy-9* mutant, an intermediate strength allele that sensitizes flowering to the endogenous rise of GA. In contrast with *lfy-9* or *rax1-1D*/+ single mutants, *rax1-1D*/+ *lfy-9* double mutants never produced flowers, consistent with the interpretation

Figure 4. (continued).

RAX1 mediates *CUC2* expression in a central domain in leaf axils. Bars = 200 μm in **(B)**, 25 μm in **(C)**, 50 μm in **(D)** to **(I)** and **(L)** to **(S)**, and 25 μm in **(J)**.
(A) Seedlings were germinated in the dark for 5 d, transferred to light, and sampled every 2 d. Ten to twenty seedlings were fixed and dissected to count leaf primordia, and ~30 seedlings were used to extract RNA for analysis of *RAX1* RNA levels by RT-PCR. Mean number of vegetative leaves (not including cotyledons) that were counted at each time point is indicated below abscissa; the number of plants evaluated at each time point is given in parentheses.
(B) to **(I)** Vegetative wild-type (Col-0) shoot apices were processed for in situ hybridization with a 707-bp specific probe.
(B) Longitudinal section of a shoot apex shows accumulation of *RAX1* RNA at the base of the adaxial side of young leaf primordia (closed arrowheads). *RAX1* is not expressed at the equivalent position in older leaf primordia (open arrowhead).
(C) Close-up of *RAX1* RNA accumulation pattern in young leaf primordium.
(D) to **(G)** Serial 8-μm cross sections of a wild-type SAM ~8 μm below the top of the SAM **(D)**, showing localized *RAX1* RNA accumulation at the center of the adaxial face of the incipient leaf primordium, ~16 μm below the top of the SAM **(E)**, ~24 μm below the top of the SAM **(F)** (outlines of leaf primordia are traced in blue), and ~32 μm below the top of the SAM **(G)**.
(H) *RAX1* expression in an early AM, recapitulating the expression pattern at the shoot apex, with *RAX1* RNA accumulation on the adaxial face of the incipient leaf primordia.
(I) Cross section of a wild-type (Col-0) shoot apex shows uniform accumulation of *CUC2* RNA along the boundary between the SAM and incipient leaf primordia (arrowheads).
(J) Cross section of a *rax1-2* shoot apex hybridized to *CUC2* antisense probe shows that the accumulation of *CUC2* RNA is interrupted at the center of boundary between the SAM and incipient leaf primordia. The gap in *CUC2* RNA accumulation (arrowhead) is precisely where *RAX1* RNA accumulates in the wild type (cf. with Figure 4F).
(K) RT-PCR analysis of *CUC2* RNA levels in shoot apices of wild-type (Ws-2) and *rax1-2* plants shows that *CUC2* accumulates to ~0.5× lower levels in the *rax1-2* background.
(L) and **(M)** Cross sections hybridized to *STM* antisense probe.
(L) Ws-2 apex ~80 μm below the top of the SAM, showing localized *STM* expression in axils at the onset of AM activation (arrowheads). Outlines of leaves are traced in blue.
(M) *rax1-2* apex ~72 μm below the top of the SAM with localized *STM* expression in axils at the onset of AM activation (arrowheads).
(N) to **(S)** Cross sections hybridized to *WUS* antisense probe.
(N) FA4C apex ~24 μm below the top, showing *WUS* expression in a central domain of the SAM.
(O) FA4C leaf axil, with focused *WUS* expression in an incipient AM. Outline of the leaf is traced in black.
(P) *rax1-1D*/+ apex ~24 μm below the top, showing *WUS* expression in a central domain of the SAM.
(Q) *rax1-1D*/+ apex ~56 μm below the top, showing *WUS* expression at axillary positions in young leaves. Note how expression is in a larger domain when compared with the wild type in **(O)** in leaves numbered 3 to 5 and the presence of two discrete foci in leaf 8. Outlines of leaves traced in black.
(R) Close-up of leaf 5 shown in **(Q)** with a large domain of *WUS* expression.
(S) Close-up of the axil of leaf 8 in **(Q)**, showing two separate zones of *WUS* expression.

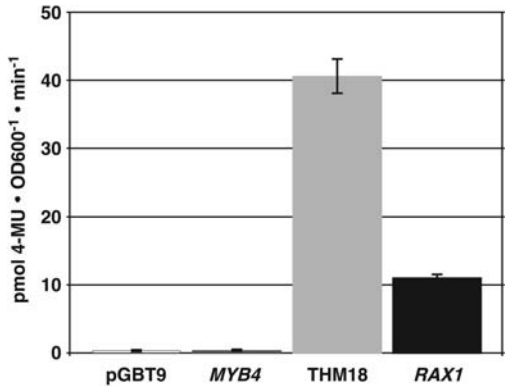

Figure 5. *RAX1* Is a Transcriptional Activator.

The magnitude of transactivation conferred by the putative *RAX1* transactivation domain C-terminal to the DBD was tested in yeast. The bars indicate the means of results obtained in quadruplicate measurements performed on each of four independently transformed yeast cultures; error bars indicate standard error of the mean. *RAX1* transactivation strength is ~25% of the strong activation conferred by THM18. 4-MU, 4-methyl umbelliferone.

that endogenous levels of GA are lower in *rax1-1D*/+ than in the wild type. Furthermore, spraying of *rax1-1D*/+ plants with GA during vegetative growth suppressed the late-flowering phenotype (see Supplemental Figure 6 online), but these plants did not produce more branches than untreated controls. The formation of the AMs was further advanced in GA-treated *rax1-1D*/+ plants (Figure 1J) than in nonsprayed plants (cf. with Figures 1H and 1I) but not sufficient for the development of a functional lateral bud that could go on to form a branch (Figure 6B). GA-treated plants frequently formed a single leaf from axillary positions (Figure 6B), suggesting that while AMs could not be sustained in this background, cell expansion mediated by GA application sufficed to generate a macroscopically visible leaf organ. Together, these data suggested that GA levels might be reduced in the *rax1-1D*/+ plants but also indicated that alleviation of this defect was insufficient to restore branching.

We then examined whether earlier flowering in *rax1-2*, specifically in SD conditions, correlated with increased GA levels using gas chromatography–mass spectrometry selected reaction monitoring (Eriksson et al., 2000). We aimed to compare GA levels late in vegetative phase, just before the transition to flowering. We also sampled Ws-2 at the time *rax1-2* flowered to compare GA levels in the early and normal flowering genotypes at this time point. Thus, we grew plants in SD conditions where inflorescences would become apparent in the rosette center of *rax1-2* and Ws-2 individuals at 42 and 46 d, respectively, and harvested samples from both genotypes at 34 d and from Ws-2 only at 40 d. Levels of the active gibberellin GA_4 were fourfold elevated in *rax1-2* compared with Ws-2 at 34 d (Figure 6C), whereas levels of GA_1, which does not induce the transition to flowering in *Arabidopsis*, were more modestly elevated (data not shown). We concluded that *RAX1* antagonizes the accumulation of GA_4, the biologically active GA required for flowering in *Arabidopsis*.

The inability to rescue branching in *rax1-1D*/+ plants sprayed with GA and the high level of GA in the *rax1-2* plants indicated that the establishment of AMs and modulation of developmental phase transitions through control of GA levels were separate functions of *RAX1*. To examine which of these functions was mediated by *CUC2* expression in the central domain of the boundary zone between the SAM and leaf primordia, *CUC2* was expressed under control of the *RAX1* promoter in a homozygous *rax1-2* background. We examined flowering time and rosette branching in lines transformed with this Pro_{RAX1}:*CUC2* construct (Table 5). Although we cannot exclude a general effect of *CUC2* expression under control of the *RAX1* promoter on flowering time or an altered expression pattern of *RAX1* in a *rax1-2* background, all eight homozygous lines examined differed significantly from the *rax1-2* background and resembled Ws-2 with respect to flowering time. Only one line, A73-10, attained wild-type levels of branching as well. This indicated that expression of *CUC2* in the *RAX1* expression domain was necessary and sufficient to control wild-type timing of flowering but not sufficient to efficiently regulate the formation of AMs.

DISCUSSION

RAX1 defines a novel genetic activity in *Arabidopsis* necessary for AM development, which also modulates the duration of vegetative development by controlling GA levels. *RAX1* is part of a small gene family of Myb-like transcription factors in *Arabidopsis* with homology to the tomato *Bl* gene, which the accompanying article shows, has distinct but complementary functions in AM formation. *RAX1* acts early in AM development and regulates *CUC2* expression in a central axillary domain that anticipates the position of future AMs. We propose that *RAX1* governs the spatial pattern of AM development by generating a tissue environment conducive for meristem establishment and therefore is involved in specifying the axillary stem cell niche.

Distinct Genetic Functions of *LAS* and *RAX1* at Organ Boundaries

Cells recruited into organ primordia rapidly initiate expression of markers such as *ASYMMETRIC LEAVES1* (Byrne et al., 2000)

Table 4. *RAX1* Modulates Vegetative Phase and Plastochron Length

Condition	Genotype (*n*)	Leaves/Day	Rosette Leaves Produced	Days to Flowering
LD	FA4C (42)	0.38	9.02 ± 0.3	23.6 ± 1.1
	rax1-1D/+ (22)	0.53*	23.1 ± 1.1*	44.2 ± 2.7*
	Ws-2 (24)	0.31	7.4 ± 0.15	23.9 ± 0.15
	rax1-2 (24)	0.32	7.6 ± 0.13	23.6 ± 0.2
SD	FA4C (50)	0.52	20.9 ± 1.4	41.8 ± 2.2
	rax1-1D/+ (18)	0.52	43.9 ± 1.8*	84.0 ± 4.6*
	Ws-2 (24)	0.54	32.3 ± 0.62	60.2 ± 0.51
	rax1-2 (22)	0.47*	25.9 ± 1.21*	54.3 ± 0.87*

Plants were grown in the photoperiod indicated. Errors are standard errors of the mean, and the asterisks indicate significant differences ($P < 0.01$) identified with Student's *t* test between mutants and the corresponding wild type. Numbers in parentheses indicate the number of individuals tested.

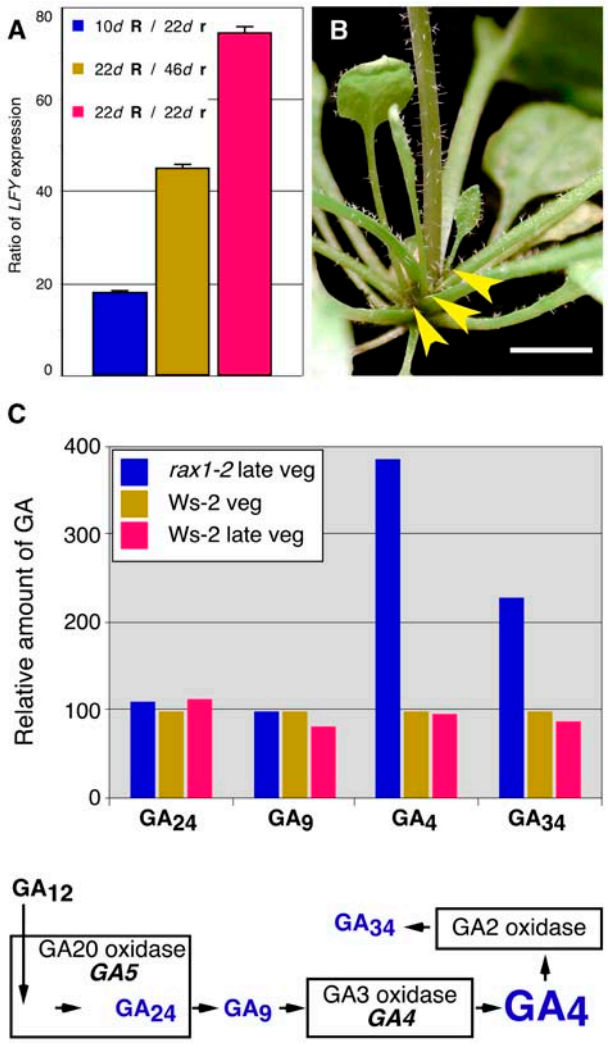

Figure 6. *RAX1* Negatively Regulates GA Accumulation.

(A) During vegetative development, *LFY* is expressed at lower levels in *rax1-1D*/+ than in FA4C plants. FA4C (*RAX1*/*RAX1*, indicated by R) and *rax1-1D*/+ (indicated by r) plants were grown in LD conditions. RNA was extracted from plants in the middle (10 d, FA4C; 22 d, *rax1-1D*/+) and late in their vegetative development (22 d, FA4C; 46 d, *rax1-1D*/+), 5 to 6 d prior to the appearance of visible inflorescences. *LFY* RNA was analyzed by RT-PCR. Expression levels were normalized to eIF4α and then ratios of normalized *LFY* expression in wild-type and *rax1-1D*/+ samples calculated.

(B) LD-grown, GA-treated *rax1-1D*/+ plants frequently produce single leaves in leaf axils (arrowheads).

(C) Top: *rax1-2* plants accumulate higher levels of GA_4 in shoot apices. Leaves larger than ~2 mm were removed, and GA levels were measured. The concentration of GA_4, which stimulates flowering in *Arabidopsis*, was approximately fourfold elevated when compared with the wild type. Bottom: schematic of the GA biosynthetic pathways showing the pathway intermediates, products, and inactive catabolites measured in *rax1-2* and wild-type plants.

and *AINTEGUMENTA* (Elliott et al., 1996), which reflect the acquisition of determinate cell fate. By contrast, cells with indeterminate fate express markers such as *STM* (Long et al., 1996). A boundary zone that straddles the morphological demarcation between SAM and primordium is defined by the expression domains of *LAS* (Greb et al., 2003), *CUC* (Takada et al., 2001), and *LOB* (Shuai et al., 2002) genes. Cells can leave this dynamic zone; therefore, cell fate is not yet fixed (Laufs et al., 2004). AMs arise from the center of this boundary zone, consistent with the observation of low-level persistence of *STM* expression in the boundary domain early during primordium development, which suggests that boundary cells are not a priori determinate (Long and Barton, 2000). It is not clear how long this competent state is maintained. *LAS* is required for subsequent, focused, high-level *STM* expression upon onset of AM development (Greb et al., 2003), suggesting that *LAS* is required for reacquisition of indeterminate cell fate in axillary cells in the course of AM organization.

By contrast, *RAX1* expression is spatially more restricted than *LAS* and is observed at a central position that anticipates the location of future AMs (Figure 4F). *RAX1* is therefore the earliest known specific marker for AM position. *RAX1* and *LAS* expression likely initiate at approximately the same stage of leaf primordium development (cf. Figures 4B and 4D to 4G with Figures 5E to 5H in Greb et al., 2003). High-level expression of *RAX1*, as observed in plants carrying the *rax1-1D* allele, which likely also somewhat expands its expression domain (Figure 2B; see Supplemental Figure 2 online), results in an enlarged zone of cells competent to initiate AMs, occasionally leading to two or more organizing centers for AM formation (Figures 1H and 1I). The expression domain of *WUS* in such incipient AMs is also expanded (Figures 4Q to 4S), suggesting higher stem cell–promoting activity. The analysis of *rax1* mutant phenotypes indicates that *RAX1* is necessary to specify AM position and sufficient to specify an AM stem cell niche within a boundary domain of cells competent to form AMs. Future experiments will determine whether *RAX1* is sufficient to specify axillary stem cell identity. Our data indicate that *RAX1* acts through *CUC2*.

Table 5. *CUC2* Expression in the *RAX1* Expression Domain in *rax1-2* Plants Restores Wild-Type Flowering Time but Not Branching

Line	*n*	Time to Flowering % of Wild Type	Rosette Paraclades % of Wild Type
Ws-2	34	100%*	100%*
rax1-2	37	92%	45%
A22-7	35	100%*	69%
A24-2	37	96%*	32%
A29-8	16	98%*	67%
A33-9	20	107%*	75%*
A41-5	20	99%*	44%
A42-17	21	108%*	41%
A63-4	19	99%*	71%
A73-10	19	101%*	99%*

Plants were grown in SD conditions. Days to flowering and rosette paraclade number were normalized to values observed for Ws-2. Data marked with asterisks are significantly different from the corresponding value of *rax1-2* ($P < 0.01$; Student's *t* test).

Interestingly, high-level expression of *CUC1* is sufficient to stimulate formation of adventitious meristems on cotyledons (Takada et al., 2001).

It is tempting to speculate on the nature of the positional cue underpinning the *RAX1* expression pattern. *REVOLUTA*, an HD-ZIP transcription factor, is required for formation of all lateral meristems (Talbert et al., 1995; Otsuga et al., 2001) and, in addition to other patterns of RNA accumulation, is expressed at adaxial positions of developing leaf primordia in a similar domain as *RAX1* (Greb et al., 2003) and therefore could generate a positional signal for *RAX1* expression. Perhaps differential accumulation of auxin directly provides a spatial cue: organogenesis requires auxin flux, which organizes a major conduit for auxin flow in the center of developing primordia (Reinhardt et al., 2003), and the *RAX1* promoter has an auxin response element. Further experiments are necessary to understand the regulation of *RAX1* expression.

Complex Phenotypes in *rax1-1D*/+ Plants

Two phenotypic aspects of the *rax1-1D*/+ plants appear paradoxical. First, while establishment of AM organizing centers is promoted (Figures 1H, 1I, and 4Q to 4S), rosette branching is highly reduced. We cannot exclude that this aspect of the *rax1-1D*/+ phenotype is neomorphic, caused by the expansion of the *RAX1* expression domain (Figure 2B; see Supplemental Figure 2 online). Ectopic *RAX1* expression might exacerbate local differences in GA levels between *rax1-1D*/+ mutants and wild-type plants. Furthermore, auxin is required for GA responses (Fu and Harberd, 2003); therefore, dynamic changes in basipetal auxin flux in the course of postembryonic development could further modify growth responses in *rax1-1D*/+ plants. Second, does our observation that the total number of branches (irrespective of their identity) in *rax1-1D*/+ compared with wild-type plants is only modestly reduced (Table 2) mean that branching is just shifted upwards in favor of cauline branches in the hemizygous mutants? Branch number is positively correlated with the length of vegetative development (Table 2, cf. Ws-2 in SD and LD). Furthermore, in *rax1-1D*/+, 0.25 ± 0.01 branches are made per leaf (rosette or cauline) on the primary stem, whereas in FA4C, 0.42 ± 0.07 branches are made. Thus, total branch number only appears similar because *rax1-1D*/+ plants have a longer vegetative phase while producing branches at a lower rate.

Is Control of Flowering Time a Direct Function of *RAX1*?

What is the significance of our observation that *RAX1* represses GA accumulation in the shoot apex (Figure 6C)? GA is required for flowering in SD-grown *Arabidopsis*: GA-biosynthetic mutants are unable to flower under these conditions (Wilson et al., 1992), while treatments with exogenous GAs restore flowering. Modulation of GA levels by *RAX1* has the effect of extending the vegetative phase, especially in SD conditions (Tables 2 and 4), which allows for the formation of more leaves and, hence, increased potential for rosette paraclade formation. Whether *RAX1* is a selfish gene that sets up a positive feedback loop to promote vegetative identity remains to be determined. Modulation of GA levels by *RAX1* could confer selective advantages if moderately late flowering in SD led to larger seed set or better dispersal by larger branch numbers.

However, GA does not only regulate flowering, but is also involved in enforcing determinate cell fate: KNOX transcription factors such as *STM* or *KNAT1* suppress GA_{20}-oxidase expression in indeterminate cells (Sakamoto et al., 2001); conversely, *spindly*, which shows constitutive GA responses, enhances the *stm* phenotype (Hay et al., 2002), suggesting that elevated GA levels or GA responses in the SAM impair indeterminacy. As GA can freely diffuse, these observations imply that low GA levels in the axillary boundary zone are critical to maintain indeterminacy of cells within it and the ability to organize AMs. Such control of GA levels in the axillary boundary could proceed by similar mechanisms as have been reported for the SAM by regulation of catabolic GA_2-oxidase expression (Jasinski et al., 2005). Therefore, the observation of early flowering in *rax1-2* could be simply a consequence of a diminished ability to block GA diffusion from developing leaf primordia to the SAM. Interestingly, our observation that restoration of *CUC2* expression in the *RAX1* expression domain in a *rax1-2* background is sufficient to completely restore wild-type timing of flowering, but only partly suppresses the branching defect (Table 5), suggests that *RAX1* has additional target genes necessary to promote AM formation and that AM formation and control of GA levels are mechanistically separable.

METHODS

Plant Materials, Mutants, and Growth Conditions

An activation-tagged collection was generated in the FA4C background (Colón-Carmona et al., 1999) using the pSKI015 vector (Weigel et al., 2000). Thermal asymmetric interlaced PCR was performed to identify sequences flanking T-DNA insertion sites, using four 35S enhancer-specific nested primers: 35S+21, 5′-ACGACACTCTCGTCTACTCCAAG-3′; 35S+53, 5′-GATACAGTCTCAGAAGACCAGAG-3′; 35S+93, 5′-AACAAAGGGTAATATCGGGAAAC-3′; and 35S+205, 5′-TAAAGGAAAGGCTATCGTTCAAG-3′ combined with the AD1, AD2, or AD3 degenerate primer (Liu et al., 1995). *rax1-2* was isolated from the α T-DNA insert population (Krysan et al., 1999) by PCR-based screening (http://www.biotech.wisc.edu/arabidopsis/). The T-DNA insertion site in *rax1-2* was identified by sequencing the PCR product amplified with the left border primer JL-202 and gene-specific primer myb37-6258: 5′-CCCATAAAACTGATCATAGTCGCTCTCTA-3′.

For genotyping, the wild-type *RAX1* and *rax1-1D* alleles were detected by PCR using primer pairs: TF2001, 5′-GGTTTAACAGCCTGGCAAAAAACTTCAG-3′, and TF2561, 5′-CGATTGCATCAATCCCTTTCTCCTACG-3′, for the wild-type *RAX1* allele and 35S+205 and TF2561 for the *rax1-1D* allele. The wild-type *RAX1* and *rax1-2* alleles were genotyped with primers myb37-4548, 5′-TCCTCCATAAACACAAAAAGTCCATCCTA-3′, and myb37-5684 for the wild-type allele and JL-202 and myb37-5684 for the *rax1-2* allele. Genotypes for *CUC1* and *CUC2* loci were determined by PCR using primers as described (Takada et al., 2001).

Prior to genetic analysis, the *rax1-1D* and *rax1-2* mutants, isolated in Col-0 or Ws-2 backgrounds, respectively, were backcrossed five times to Landsberg *erecta* or Col-0. *rax1-2* was crossed into *cuc1*/*cuc1 cuc2*/+, all in the Landsberg *erecta* background.

Rosette branches were scored ~3 weeks after onset of inflorescence stem elongation by visual inspection of individual plants. Only secondary growth axes elongated more than 5 mm were scored.

Plants were grown under LD (16 h light/8 h dark) or SD (9 h light/15 h dark) conditions in controlled environment rooms at 21°C on shelves with an average of 120 μE m^{-2} s^{-1} fluorescent light.

Plasmid Construction and Plant Transformation

All constructs were verified by DNA sequencing. To recapitulate the *rax1-1D* phenotype, genomic DNA was PCR amplified, comprising 4x35S enhancer elements, ~2.3 kb 5′ of the *RAX1* start codon, the entire coding region, including introns, and ~0.6 kb 3′ untranslated region, and subsequently transformed into Col-0 plants. To complement *rax1-2*, the PCR-amplified transgene consisted of ~1.9 kb 5′ of the *RAX1* start codon, the entire coding region, including introns, and ~0.6 kb of the 3′ untranslated region. To construct a Pro_{RAX1}:*CUC2* fusion, an ~2.1-kb genomic fragment encompassing the putative *RAX1* promoter was amplified with primers myb37-2507 (5′-GTCGACAACATTACAACTCAAGGGCAGACG-3′) and myb37-4669 (5′-CACCCTAGGCTTCCCATTTCTCTCGTTAGTG-3′) and digested with *Sal*I and *Avr*II. CUC2 was isolated as an ~2.2-kb genomic *Nco*I-*Eco*RI fragment. These fragments were ligated together after addition of an *Avr*II-*Nco*I linker and introduced into the $pSPTV50^{hyg}$ plant transformation vector. The final construct was transformed into Col-0 plants via the *Agrobacterium tumefaciens*–mediated floral dip method (Clough and Bent, 1998).

Yeast Constructs and Methods

For *RAX1*, a cDNA fragment corresponding to amino acids 119 to 329 was cloned in frame downstream of the GAL4 DBD of the yeast expression vector pGBT9 (Clontech). The activation control construct $GAL4_{DBD}$:*THM18* with sequences encoding amino acids 163 to 256 of THM18 (Schwechheimer et al., 1998) and the repression control construct $GAL4_{DBD}$:*MYB4* with sequences encoding amino acids 163 to 282 of MYB4 (Jin et al., 2000) were made in a similar way. Yeast strain HF7c (Clontech) was transformed by the LiAc method (http://www.umanitoba.ca/faculties/medicine/biochem/gietz/).

The protocol for liquid culture β-galactosidase assays in yeast (Clontech; Yeast Protocol Handbook PT3024-1) was modified for use with 4-methyl umbelliferyl β-D-galactopyranoside as a substrate. After assay for 15 min at 30°C, the fluorescent product, 4-methyl umbelliferone, was detected in a spectrofluorometer (BMG Labtechnologies) using excitation and emission wavelengths of 360 and 460 nm, respectively. Enzyme activity was calculated as the amount of 4-methyl umbelliferone produced per OD_{600} per minute. This assay was repeated on four independently transformed lines.

GA Treatments and Quantification of Endogenous GA

Application of exogenous GA_3 (G-7645; Sigma-Aldrich) during vegetative growth under LD and SD conditions was achieved by spraying soil-grown plants twice weekly with a solution of 100 μM GA_3 and 0.02% Tween-20. Control plants were treated with the same concentration of surfactant in water. For GA measurements, shoot apices were microdissected by hand to remove all leaf primordia >2mm, stem segments, and roots. Endogenous GAs were extracted from apices and analyzed by gas chromatography–tandem mass spectrometry (JMS-MStation 700; JEOL) using $^2H_2$-labeled GAs (L. Mander, Canberra, Australia) as internal standards as described (Eriksson et al., 2000). Averaged GA values were normalized to GA concentrations in vegetative apices of corresponding lines.

RNA Analysis, RT-PCR, and Quantitative PCR

RNA was isolated from apices and leaves using Trizol reagent (Invitrogen). For RNA gel blot analysis, 20 μg total RNA was separated by electrophoresis, transferred to Hybond N^+ nylon membranes, hybridized, and washed following standard procedures (Ausubel et al., 1987). A *RAX1*-specific cDNA probe was amplified with primers TF258, 5′-AGGAAGCAGGTGGTCAATAATAGC-3′, and TF759, 5′-CCTTTTGTCCTCTGGTCAATGTGG-3′. RNA loading was checked by hybridization to *eIF-4A* transcripts.

Reverse transcription reactions were done with 1 μg of total RNA and 250 ng oligo(dT) or 10 pmol gene-specific primers in 10-μL reactions according to the manufacturer's protocol (ABgene). Diluted aliquots of the resulting reverse transcription reaction products were used for quantitative PCR (Q-PCR) analysis. Q-PCR was performed in an iCycler (Bio-Rad) using SYBR Green I (Molecular Probes) and ABsolute QPCR mix (ABgene) with 40 ng primers in a total of 20 μL per reaction. Quadruplicate Q-PCR reactions were averaged. The following primer pairs were used for *RAX1* (At5g23000): myb37-4997, 5′-GCCATAGGAAGCAGGTGGTC-3′, and myb37-5593, 5′-GGGATTGTTGTTGGTGAGGT-3′, or myb37-5684, 5′-GTCACCAGCTTCGAAGCCATTG-3′. To confirm the absence of a truncated *RAX1* transcript upstream of the T-DNA insertion in *rax1-2*, the primer pair myb37 5′ RT1, 5′-ACTTAGAGATTACATTGAAAAGTATGGT-3′, and myb37 5′ RT2, 5′-CAGCGAAGAGACTAAAAATGATC-3′, was used. Other specific primers were as follows: CUC2-243, 5′-GAAGTATCCGACGGGACTGA-3′, and CUC2-487, 5′-GATCACCCATTCATCCTTGGAG-3′, for *CUC2* (At5g53950) and eIFT22, 5′-TTCGCTCTTCTCTTTGCTCTC-3′, and eIFB221, 5′-GAACTCATCTTGTCCCTCAAGTA-3′, for *eIF-4A* (At3g13920). Relative transcript levels in all samples were normalized using *eIF-4A*. A no-template control was included in each set of reactions to confirm the absence of contamination. The primers spanned at least one intron to distinguish cDNA amplification products from genomic DNA contamination.

In Situ Hybridization

Shoot apices were fixed in *p*-formaldehyde, paraffin embedded, sectioned to 8 μm, affixed to Probe Plus slides (Fisher Scientific) at 42°C overnight, and processed as described (http://www-ciwdpb.stanford.edu/research/barton/in_situ_protocol.html) with color substrate incubation overnight. For probes, a 707-bp *RAX1* fragment was amplified with gene-specific primers myb37-5551, 5′-TTTCTCAGGATGTGAAAAGACCAACC-3′, and myb37-6258, 5′-CCCATAAAACTGATCATAGTCGCTCTCTA-3′; a 627-bp *CUC2* template was synthesized with primers CUC2-1703, 5′-CCAGAAAACCACTTTAGCTAGC-3′, and CUC2-2330, 5′-TCAGTAGTTCCAAATACAGTCAA-3′; a 545-bp *STM* fragment was amplified from cDNA with primers stm-1, 5′-ATGGAGAGTGGTTCCAACAG-3′, and stm-1505, 5′-GATCAAGCCCTGGATCTTCA-3′; and a full-length cDNA generated from pMH16 was used as *WUS* probe (a gift from Martin Hobe). Fragments were cloned in sense and antisense orientation into pGEM-Teasy (Promega), and probes were synthesized by T7 RNA polymerase.

Phylogenetic Analysis

Conceptually translated cDNA sequences corresponding to the conserved DBD were aligned using ClustalW in the Lasergene suite (DNAStar) (see Supplemental Figure 7 online). The alignment file was used to generate a phylogenetic tree and to calculate the posterior probabilities of nodes with the Bayesian method implemented in MrBayes3.0 (Ronquist and Huelsenbeck, 2003; http://mrbayes.csit.fsu.edu/index.php). The program was run with the default settings for 100,000 generations.

Accession Numbers

Sequence data from this article can be found in the GenBank/EMBL data libraries under accession numbers AK175507 (MYB37), AJ012310 (*WUS*), NM_124774 (*CUC2*), AF543194 (*CUC3*), and NM_104434 (*LAS*).

Supplemental Data

The following materials are available in the online version of this article.

Supplemental Figure 1. Flower Number in Wild-Type, *rax1-1D*/+, and *rax1-2* Plants.

Supplemental Figure 2. *RAX1* Is Ectopically Expressed in *rax1-1D*/+ Leaves.

Supplemental Figure 3. *RAX1* Transcripts Do Not Accumulate in *rax1-2*.

Supplemental Figure 4. Expression of *LAS* and *CUC3* in *rax1-1D*/+ Shoot Apices

Supplemental Figure 5. The Juvenile Phase of Vegetative Development Is Not Altered in *rax1* Mutants.

Supplemental Figure 6. GA Sprays during Vegetative Development Suppress Late Flowering in *rax1-1D*/+ Plants.

Supplemental Figure 7. ClustalW Alignment of *Arabidopsis* and Tomato Myb Genes.

ACKNOWLEDGMENTS

We thank Shalu Mittal, Ratha You, Heng Phung, and Tal Heimovitch-Gal for help in generating the activation-tagged collection in the FA4C background. We also thank Marc Morgan, Stephanie Albouhair, Lydia Barth, Bavani Krishnan, and Angie Ng Ah Sock for help with characterizing the *rax1* mutants. We thank Chris Jeffries for help with scanning electron microscopy analysis. We thank Ken-ichiro Hibara for seeds of the *cuc1*/*cuc1 cuc2*/+ mutant, Cathie Martin for the $GAL4_{DBD}$:*THM18* and $GAL4_{DBD}$:At *MYB4* clones and the Nottingham Arabidopsis Stock Centre for seed of various mutants. This work was supported by grants from Akkadix and the Biotechnology and Biological Science Research Council.

Received October 10, 2005; revised December 15, 2005; accepted January 17, 2006; published February 10, 2006.

REFERENCES

Aida, M., Ishida, T., and Tasaka, M. (1999). Shoot apical meristem and cotyledon formation during *Arabidopsis* embryogenesis: Interaction among the CUP-SHAPED COTYLEDON and SHOOT MERISTEMLESS genes. Development **126,** 1563–1570.

Alonso, J.M., et al. (2003). Genome-wide insertional mutagenesis of *Arabidopsis thaliana.* Science **301,** 653–657.

Ausubel, F.M., Brent, R., Kingston, R.E., More, D.D., Seidman, J.G., Smith, J.A., and Struhl, K. (1987). Current Protocols in Molecular Biology. (New York: Greene Publishing Associates and Wiley-Interscience).

Blazquez, M.A., Green, R., Nilsson, O., Sussman, M.R., and Weigel, D. (1998). Gibberellins promote flowering of *Arabidopsis* by activating the *LEAFY* promoter. Plant Cell **10,** 791–800.

Byrne, M.E., Barley, R., Curtis, M., Arroyo, J.M., Dunham, M., Hudson, A., and Martienssen, R.A. (2000). Asymmetric leaves1 mediates leaf patterning and stem cell function in *Arabidopsis.* Nature **408,** 967–971.

Cline, M.G. (1997). Concepts and terminology of apical dominance. Am. J. Bot. **84,** 1064–1069.

Clough, S.J., and Bent, A.F. (1998). Floral dip: A simplified method for *Agrobacterium*-mediated transformation of *Arabidopsis thaliana.* Plant J. **16,** 735–743.

Colón-Carmona, A., You, R., Haimovitch-Gal, T., and Doerner, P. (1999). Technical advance: Spatio-temporal analysis of mitotic activity with a labile cyclin-GUS fusion protein. Plant J. **20,** 503–508.

Daimon, Y., Takabe, K., and Tasaka, M. (2003). The CUP-SHAPED COTYLEDON genes promote adventitious shoot formation on calli. Plant Cell Physiol. **44,** 113–121.

Doerner, P. (2003). Plant meristems: A merry-go-round of signals. Curr. Biol. **13,** R368–R374.

Elliott, R.C., Betzner, A.S., Huttner, E., Oakes, M.P., Tucker, W.Q., Gerentes, D., Perez, P., and Smyth, D.R. (1996). AINTEGUMENTA, an APETALA2-like gene of Arabidopsis with pleiotropic roles in ovule development and floral organ growth. Plant Cell **8,** 155–168.

Eriksson, M.E., Israelsson, M., Olsson, O., and Moritz, T. (2000). Increased gibberellin biosynthesis in transgenic trees promotes growth, biomass production and xylem fiber length. Nat. Biotechnol. **18,** 784–788.

Feng, C., Andreasson, E., Maslak, A., Mock, H.P., Mattsson, O., and Mundy, J. (2004). Arabidopsis MYB68 in development and responses to environmental cues. Plant Sci. **167,** 1099–1107.

Fu, X., and Harberd, N.P. (2003). Auxin promotes *Arabidopsis* root growth by modulating gibberellin response. Nature **421,** 740–743.

Gallois, J.L., Woodward, C., Reddy, G.V., and Sablowski, R. (2002). Combined SHOOT MERISTEMLESS and WUSCHEL trigger ectopic organogenesis in Arabidopsis. Development **129,** 3207–3217.

Grbic, V., and Bleecker, A.B. (2000). Axillary meristem development in *Arabidopsis thaliana.* Plant J. **21,** 215–224.

Greb, T., Clarenz, O., Schafer, E., Muller, D., Herrero, R., Schmitz, G., and Theres, K. (2003). Molecular analysis of the *LATERAL SUPPRESSOR* gene in *Arabidopsis* reveals a conserved control mechanism for axillary meristem formation. Genes Dev. **17,** 1175–1187.

Green, K.A., Prigge, M.J., Katzman, R.B., and Clark, S.E. (2005). CORONA, a member of the class III homeodomain leucine zipper gene family in *Arabidopsis*, regulates stem cell specification and organogenesis. Plant Cell **17,** 691–704.

Haecker, A., Gross-Hardt, R., Geiges, B., Sarkar, A., Breuninger, H., Herrmann, M., and Laux, T. (2004). Expression dynamics of WOX genes mark cell fate decisions during early embryonic patterning in *Arabidopsis thaliana.* Development **131,** 657–668.

Hay, A., Kaur, H., Phillips, A., Hedden, P., Hake, S., and Tsiantis, M. (2002). The gibberellin pathway mediates KNOTTED1-type homeobox function in plants with different body plans. Curr. Biol. **12,** 1557–1565.

Hempel, F.D., and Feldman, L.J. (1994). Bi-directional inflorescence development in *Arabidopsis thaliana*: Acropetal initiation of flowers and basipetal initiation of paraclades. Planta **192,** 276–286.

Jasinski, S., Piazza, P., Craft, J., Hay, A., Woolley, L., Rieu, I., Phillips, A., Hedden, P., and Tsiantis, M. (2005). KNOX action in *Arabidopsis* is mediated by coordinate regulation of cytokinin and gibberellin activities. Curr. Biol. **15,** 1560–1565.

Jin, H., Cominelli, E., Bailey, P., Parr, A., Mehrtens, F., Jones, J., Tonelli, C., Weisshaar, B., and Martin, C. (2000). Transcriptional repression by AtMYB4 controls production of UV-protecting sunscreens in Arabidopsis. EMBO J. **19,** 6150–6161.

Krysan, P.J., Young, J.C., and Sussman, M.R. (1999). T-DNA as an insertional mutagen in *Arabidopsis.* Plant Cell **11,** 2283–2290.

Laufs, P., Peaucelle, A., Morin, H., and Traas, J. (2004). MicroRNA regulation of the CUC genes is required for boundary size control in *Arabidopsis* meristems. Development **131,** 4311–4322.

Lenhard, M., Jurgens, G., and Laux, T. (2002). The *WUSCHEL* and *SHOOTMERISTEMLESS* genes fulfil complementary roles in *Arabidopsis* shoot meristem regulation. Development **129,** 3195–3206.

Liu, Y.G., Mitsukawa, N., Oosumi, T., and Whittier, R.F. (1995). Efficient isolation and mapping of *Arabidopsis thaliana* T-DNA insert junctions by thermal asymmetric interlaced PCR. Plant J. **8,** 457–463.

Long, J., and Barton, M.K. (2000). Initiation of axillary and floral meristems in *Arabidopsis*. Dev. Biol. **218,** 341–353.

Long, J.A., Moan, E.I., Medford, J.I., and Barton, M.K. (1996). A member of the KNOTTED class of homeodomain proteins encoded by the STM gene of Arabidopsis. Nature **379,** 66–69.

McSteen, P., and Leyser, O. (2005). Shoot branching. Annu. Rev. Plant Biol. **56,** 353–374.

Otsuga, D., DeGuzman, B., Prigge, M.J., Drews, G.N., and Clark, S.E. (2001). REVOLUTA regulates meristem initiation at lateral positions. Plant J. **25,** 223–236.

Reinhardt, D., Pesce, E.R., Stieger, P., Mandel, T., Baltensperger, K., Bennett, M., Traas, J., Friml, J., and Kuhlemeier, C. (2003). Regulation of phyllotaxis by polar auxin transport. Nature **426,** 255–260.

Ronquist, F., and Huelsenbeck, J.P. (2003). MrBayes 3: Bayesian phylogenetic inference under mixed models. Bioinformatics **19,** 1572–1574.

Sakamoto, T., Kamiya, N., Ueguchi-Tanaka, M., Iwahori, S., and Matsuoka, M. (2001). KNOX homeodomain protein directly suppresses the expression of a gibberellin biosynthetic gene in the tobacco shoot apical meristem. Genes Dev. **15,** 581–590.

Schmitz, G., and Theres, K. (2005). Shoot and inflorescence branching. Curr. Opin. Plant Biol. **8,** 506–511.

Schmitz, G., Tillmann, E., Carriero, F., Fiore, C., Cellini, F., and Theres, K. (2002). The tomato Blind gene encodes a MYB transcription factor that controls the formation of lateral meristems. Proc. Natl. Acad. Sci. USA **99,** 1064–1069.

Schwechheimer, C., Smith, C., and Bevan, M.W. (1998). The activities of acidic and glutamine-rich transcriptional activation domains in plant cells: Design of modular transcription factors for high-level expression. Plant Mol. Biol. **36,** 195–204.

Shuai, B., Reynaga-Pena, C.G., and Springer, P.S. (2002). The lateral organ boundaries gene defines a novel, plant-specific gene family. Plant Physiol. **129,** 747–761.

Simpson, G.G., and Dean, C. (2002). *Arabidopsis*, the Rosetta stone of flowering time? Science **296,** 285–289.

Snow, M., and Snow, R. (1942). The determination of axillary buds. New Phytol. **41,** 13–22.

Stirnberg, P., Chatfield, S.P., and Leyser, H.M. (1999). AXR1 acts after lateral bud formation to inhibit lateral bud growth in *Arabidopsis.* Plant Physiol. **121,** 839–847.

Stirnberg, P., van de Sande, K., and Leyser, H.M.O. (2002). MAX1 and MAX2 control shoot lateral branching in *Arabidopsis.* Development **129,** 1131–1141.

Stracke, R., Werber, M., and Weisshaar, B. (2001). The R2R3-MYB gene family in *Arabidopsis thaliana.* Curr. Opin. Plant Biol. **4,** 447–456.

Sussex, I.M. (1955). Morphogenesis in *Solanum tuberosum* L: Experimental investigation of leaf dorsoventrality and orientation of the juvenile shoot. Phytomorphology **5,** 286–300.

Takada, S., Hibara, K., Ishida, T., and Tasaka, M. (2001). The CUP-SHAPED COTYLEDON1 gene of *Arabidopsis* regulates shoot apical meristem formation. Development **128,** 1127–1135.

Talbert, P.B., Adler, H.T., Parks, D.W., and Comai, L. (1995). The REVOLUTA gene is necessary for apical meristem development and for limiting cell divisions in the leaves and stems of *Arabidopsis thaliana.* Development **121,** 2723–2735.

Telfer, A., Bollman, K.M., and Poethig, R.S. (1997). Phase change and the regulation of trichome distribution in *Arabidopsis thaliana.* Development **124,** 645–654.

Weigel, D., et al. (2000). Activation tagging in *Arabidopsis.* Plant Physiol. **122,** 1003–1013.

Wilson, R.N., Heckman, J.W., and Somerville, C.R. (1992). Gibberellin is required for flowering in *Arabidopsis thaliana* under short days. Plant Physiol. **100,** 403–408.